Chapter 1

Carbonate clumped isotopes in sedimentary rocks: Insights from the Sultanate of Oman

Kristin D. Bergmann[1], Said Al Balushi[2], John P. Grotzinger[1], John M. Eiler[1]

[1]California Institute of Technology

[2]Petroleum Development Oman

1.1 Abstract

While the field of carbonate clumped isotope thermometry has grown dramatically since its recent inception [1, 2, 3, 4], there remains considerable uncertainty regarding its usefulness in questions of deep time. This is in large part because questions remain regarding the impact of burial on the isotopic ordering within the carbonate crystal lattice. There is evidence that both recrystallization and solid state diffusion within the crystal lattice are important processes [5, 6, 3, 7, 8]. Yet the time and depth dependence of these processes remains poorly constrained in natural samples. This study explores how the burial and exhumation history modifies the primary ordering of ^{13}C and ^{18}O in carbonates from the subsurface and surface of Oman. The study suite includes carbonates of Eocene to Neoproterozoic age that sit at current burial depths of 350 m to 5850 m. We can directly compare the measured clumped isotope temperatures to current borehole temperatures and

the petrography of core samples. Additionally, we analyzed exhumed carbonates from the same formations, estimated to have been buried from 1–2 km up to 8–10 km.

Results indicate two dominant modes of diagenesis within the shallow burial environment (< 6 km) that are independent of burial depth. These modes have specific temperatures in clumped isotope space as well as in reconstructed water space, calculated from the measured clumped isotope temperature and $\delta^{18}O_{min}$. One group of carbonates measured from the subsurface yield $\delta^{18}O_{water}$ compositions similar to the composition of seawater today of around 0‰ VSMOW. The Phanerozoic samples with water compositions similar to today yield clumped isotope temperatures of $< 40°C$. The Neoproterozoic samples yielding seawater-like compositions are $< 55°C$. These samples generally show excellent to moderate primary preservation of fossils and grains and clear porosity-occluding cements or microcrystalline micrite. The second mode of diagenesis found in these shallow burial environments is strongly controlled by low-water-to-rock diagenesis. Samples sit close to the current geothermal gradient, are both dolomite and calcite mineralogies, and can exhibit secondary grain coarsening. Samples exhumed at the surface from estimated shallow burial environments show both diagenetic trends while samples exhumed from greater depths (> 8 km) yield higher maximum temperatures (120–150°C) and very enriched fluid compositions (~ 8‰).

1.2 Introduction

The carbonate clumped isotope thermometer has the potential to provide new insights into the diagenetic processes dominant in the transformation of carbonate sediments into rocks. Importantly, clumped isotope thermometry allows us to estimate the absolute temperature of carbonate precipitation, including recrystallization, based on the temperature dependent abundance of carbonate ions containing both ^{13}C and ^{18}O [4]. These estimates are accompanied by a measurement of carbonate $\delta^{18}O_{min}$, which in conjunction with temperature, can be used to calculate the oxygen isotopic composition of the fluid from which the carbonate precipitated ($\delta^{18}O_{fluid}$). The thermometer has the potential to reconstruct climatic events and deconvolve the ice volume and temperature record through time. There are also numerous potential diagenetic applications for a proxy that directly measures the crystallization temperature of distinct carbonate phases and can thus independently constrain source fluid composition. These applications could include studies of cement stratigraphy, dolomitization, regional burial history, and hydrothermal alteration events (Fig. 1.2) [9, 10, 11, 12]. However, basic questions remain involving the alteration of the clumped isotopic system during carbonate burial and lithification (Fig. 1.1). While 'solid state reordering'—reordering through exchange to reflect equilibration at higher temperatures during burial without recrystallizing the solid—of the clumped isotopic signature is likely important at high temperatures it is unclear whether this process is active at lower temperatures over geologic timescales [5]. Additionally, the impact of well recognized carbonate diagenetic processes—compaction, cementation and porosity occlusion, dissolution, reprecipitation, dolomitization—on the clumped isotope thermometer remains poorly constrained.

The trajectory from primary and diagenetic processes can be mapped in a 3-plot diagram of clumped isotope temperature, $\delta^{18}O_{min}$, and $\delta^{18}O_{water}$ (Fig. 1.2). Primary processes like heating and cooling events and basin restriction and deglaciation produce a vector within this 3-plot diagram that is characteristic of a given process. For example, basin restriction or an increase in glacial ice will yield enriched fluid compositions, enriched $\delta^{18}O_{min}$ and near constant temperatures (Fig. 1.2, light blue arrow). In a similar way diagenetic processes also create an array in the 3-plot diagram. For example low water-rock ratio interactions (orange arrow)—when the $\delta^{18}O_{min}$ buffers the small pore volumes of fluid— result in increasing temperatures, constant $\delta^{18}O_{min}$ and enriched $\delta^{18}O_{fluid}$. Whereas high water-rock ratio interactions (purple and green arrows), yield constant $\delta^{18}O_{fluid}$ compositions, higher temperatures and lighter $\delta^{18}O_{min}$ (Fig. 1.2).

The stratigraphy of Oman represents a self-contained case study to explore

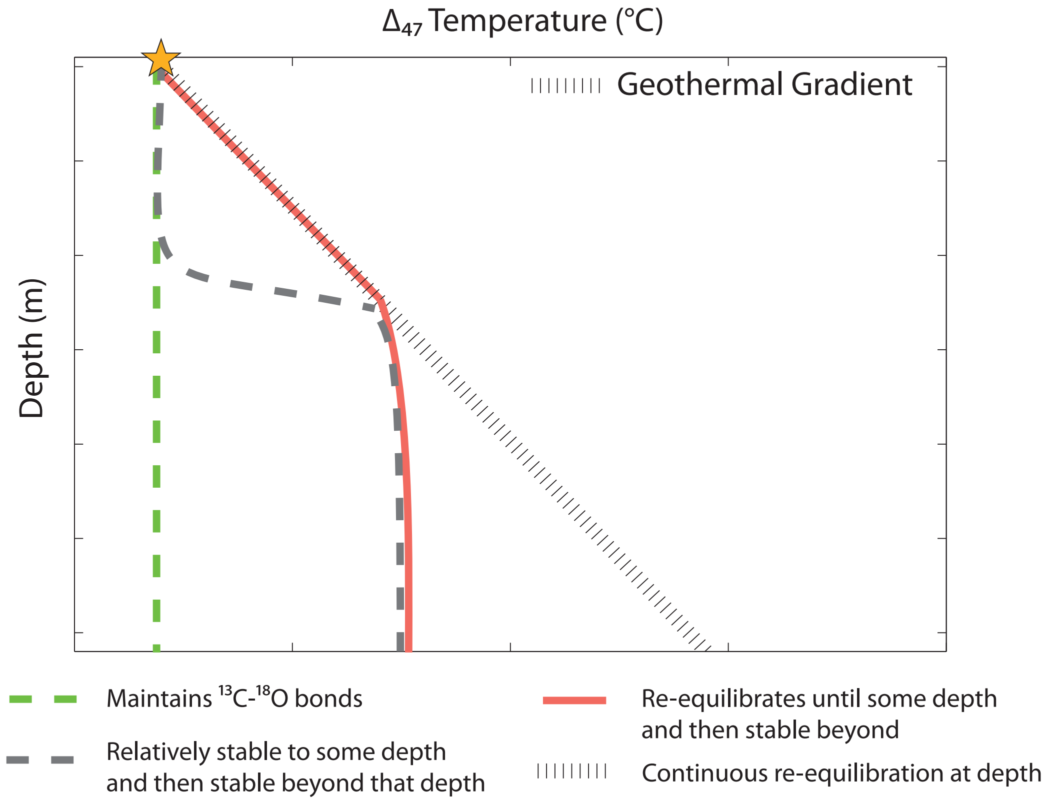

Figure 1.1: Clumped isotope temperature model during burial. Clumped isotope groups may be recalcitrant to alteration (green), alter after some burial depth and then maintain the new clumped bonding arrangement (grey), continuously alter until some depth (red) or continuously alter during burial (dashed)

the interplay between diagenetic alteration, basin development and hydrocarbon formation (Fig. 1.3). The Eocene- to Permian-aged carbonates that blanket the shallow subsurface of Oman, the Precambrian-Cambrian boundary spanning Ara Group and the Ediacaran-aged Nafun Group are broadly very different in character. The Eocene-Permian carbonates are shallowly buried in central Oman and the youngest samples remain poorly cemented. In general samples are from thick carbonate platform sequences but a few samples are from mixed siliciclastic-carbonate units. In contrast, the Ara Group is generally composed of carbonates interbedded with evaporites. Today the Ara Group carbonate ’stringers’ of the Ara Group float in the salt and are lithostatically pressured. The Nafun Group is a mixed carbonate-siliciclastic deposit composed of two grand cycles of siliciclastics tran-

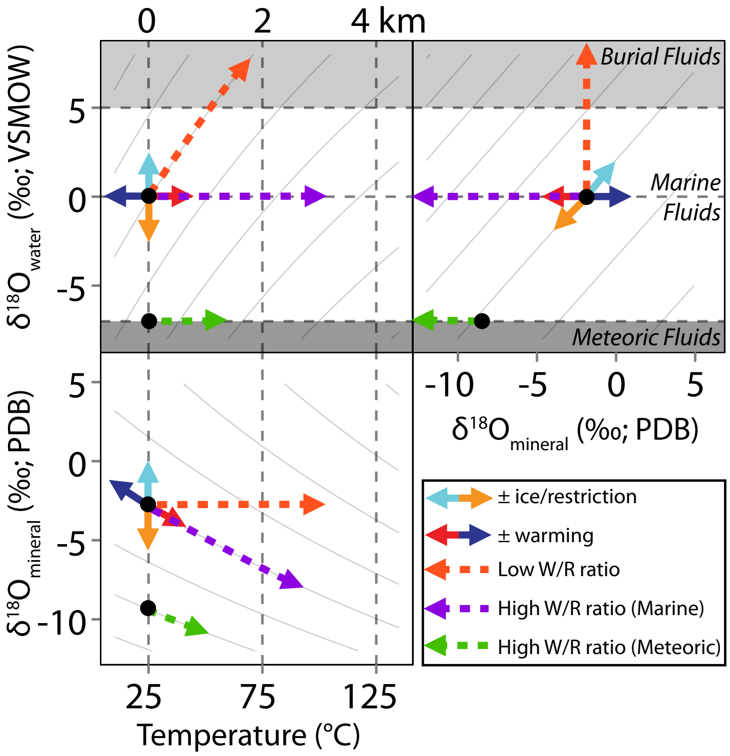

Figure 1.2: Diagenetic and primary trajectories in T, $\delta^{18}O_{min}$, $\delta^{18}O_{water}$ space. A given process (i.e., temperature change or recrystallization in the presence of enriched pore fluids) will create a specific array that can be tracked in each of the three plots.

sitioning into carbonates. The lower cycle includes the Masirah Bay and Khufai Formations and the upper cycle the Shuram and Buah formations.

To examine the variability of the clumped isotope thermometer and fluid composition with depth in the carbonate rocks of Oman, a range of burial environments were targeted. Samples were analyzed from the South Oman Salt Basin, the Eastern Flank of the South Oman Salt Basin, the Central Oman High, and salt domes accessing the Ghaba Salt Basin. Each of these regions has a different burial history that has the potential to leave an imprint on the carbonate clumped isotope thermometer. The Eocene- to Permian-aged samples off the Central Oman High have been buried 350—1400 meters. The Ara and Nafun Groups in the South Oman Salt Basin and Eastern Flank have generally been buried between 1–4 km but some samples have been buried as deep as ∼ 6 km. The Salt Domes sourcing the Ghaba Salt Basin are bringing up carbonates that have been buried ∼ 9 km.

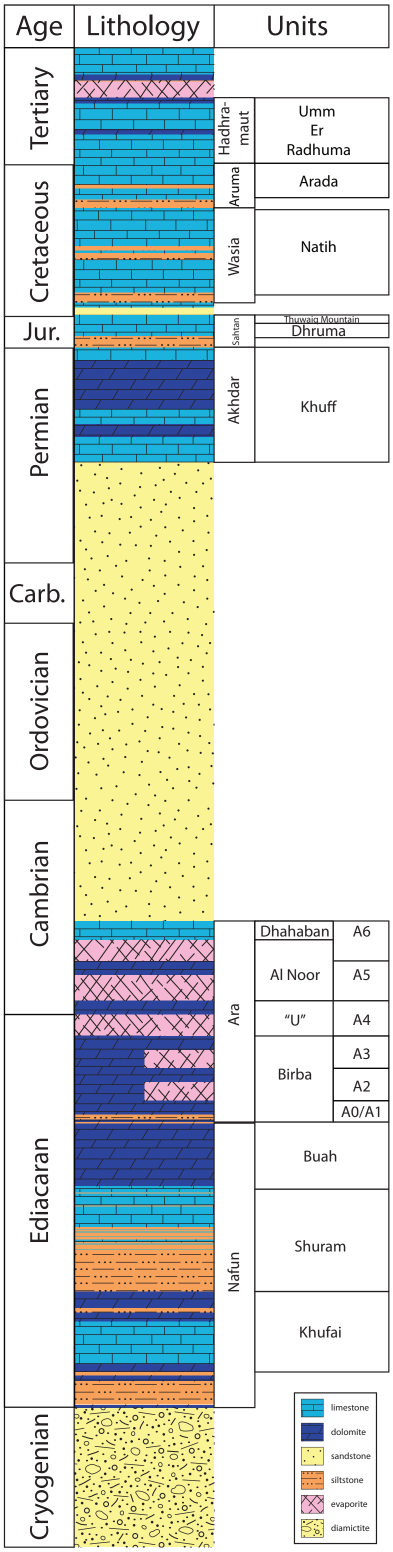

Figure 1.3: Generalized stratigraphy of Central and Southern Oman. The formations analyzed in this study are labeled on the right.

The Nafun Group on the Central Oman High in the Huqf outcrop area has the smallest overburden for the Precambrian carbonates (1–3 km) because it has been a structural high through its history (Fig. 1.4).

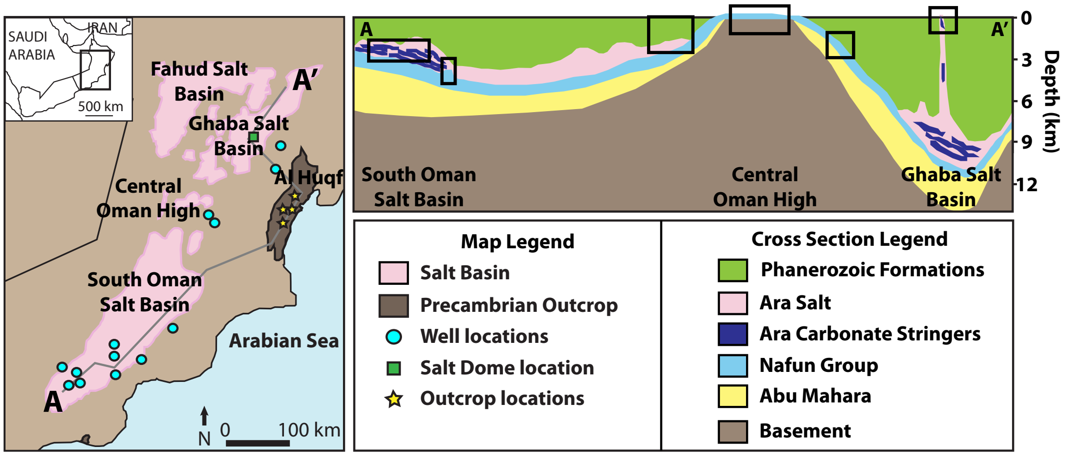

Figure 1.4: Cross sectional profile of Central and Southern Oman. The South Oman Salt Basin (SOSB) is at a shallower depth than the Ghaba Salt Basin and they are separated by the Central Oman High.

1.3 Geologic setting and sample description

1.3.1 Eocene- to Permian-aged carbonates

The record of Phanerozoic carbonate deposits in Oman exists from the Permian to present. The Khuff Formation is the first carbonate formation deposited in Oman after rifting of the Pangean supercontinent [13]. A passive margin developed in the Neo-Tethys Ocean on the Arabian Plate that led to extensive carbonate deposition within the Permian- to Cretaceous-aged Akhdar, Sahtan, Kahmah and Wasia Groups. The closure of the Neo-Tethys in the Late Cretaceous led to deformation and obduction in North Oman of the deep water Hawasina Group and the Semail Ophiolite [13]. The Hadhramaut Group blanketed the Arabian plate during the Paleocene and Eocene. Younger deposits are isolated in smaller regions across Arabia and were not sampled for this study. A single well from the Central Oman High was selected that contains these Phanerozoic carbonate units at shallow burial depths.

The youngest unit sampled, the Umm Er Radhuma Formation of the Hadhramaut Group is Eocene to Paleocene in age. The samples analyzed from this formation are fossiliferous wackestone and packestone with benthic foraminifera bioclasts. There is some intragranular calcite in the youngest sample recovered at 357 meters depth but it is generally very poorly cemented as evidenced by the visible blue stained epoxy (Fig. 1.5a, Fig. 1.6)(HM1). A nearby mold of a large gastropod $\sim$ 6 cm in width was sampled including the calcite spar infilling the interval cavity (HM2). The third sample (HM3) recovered from 414.5 meters depth contains more calcite spar but is also poorly cemented with well-preserved fossil tests (Fig. 1.5b).

Two Cretaceous-aged carbonate formations were sampled including the Arada Member of the Aruma Group and the Natih Formation of the Wasia Group. The Arada Member samples recovered from 500.3 and 500.8 meters depth are Campanian in age and are light grey wackestone with little to no primary porosity remaining (HM4 and HM5)(Fig. 1.5c,d). The fossils are filled or replaced with calcite spar and the matrix has small rhombohedral dolomite crystals in both samples (Fig. 1.6c). Calcite spar from a void was sampled from HM5 (Fig. 1.5d). The Natih Formation of the Wasia Group is Late Albian to Early Turonian in age and includes diagnostic large benthic foraminifera including *Preaealveolina cretecea* (Fig. 1.5g). The samples from the Natih A/B members recovered from 583 and 650 meters depth are packstone with many bioclasts that have been filled or replaced by calcite spar (Fig. 1.5e,f). The samples from the Natih C/E members recovered from 729.5 and 794.2 meters depth are wackestone with fewer smaller bioclasts (HM8 and HM9) (Fig. 1.5g,h). A calcite spar fracture was micro-sampled from HM8 (Fig. 1.5i). The sample from the Natih F/G members recovered from 879.5 meters depth is a packstone composed of larger bivalve shells in a micrite matrix (HM10) (Fig. 1.5l).

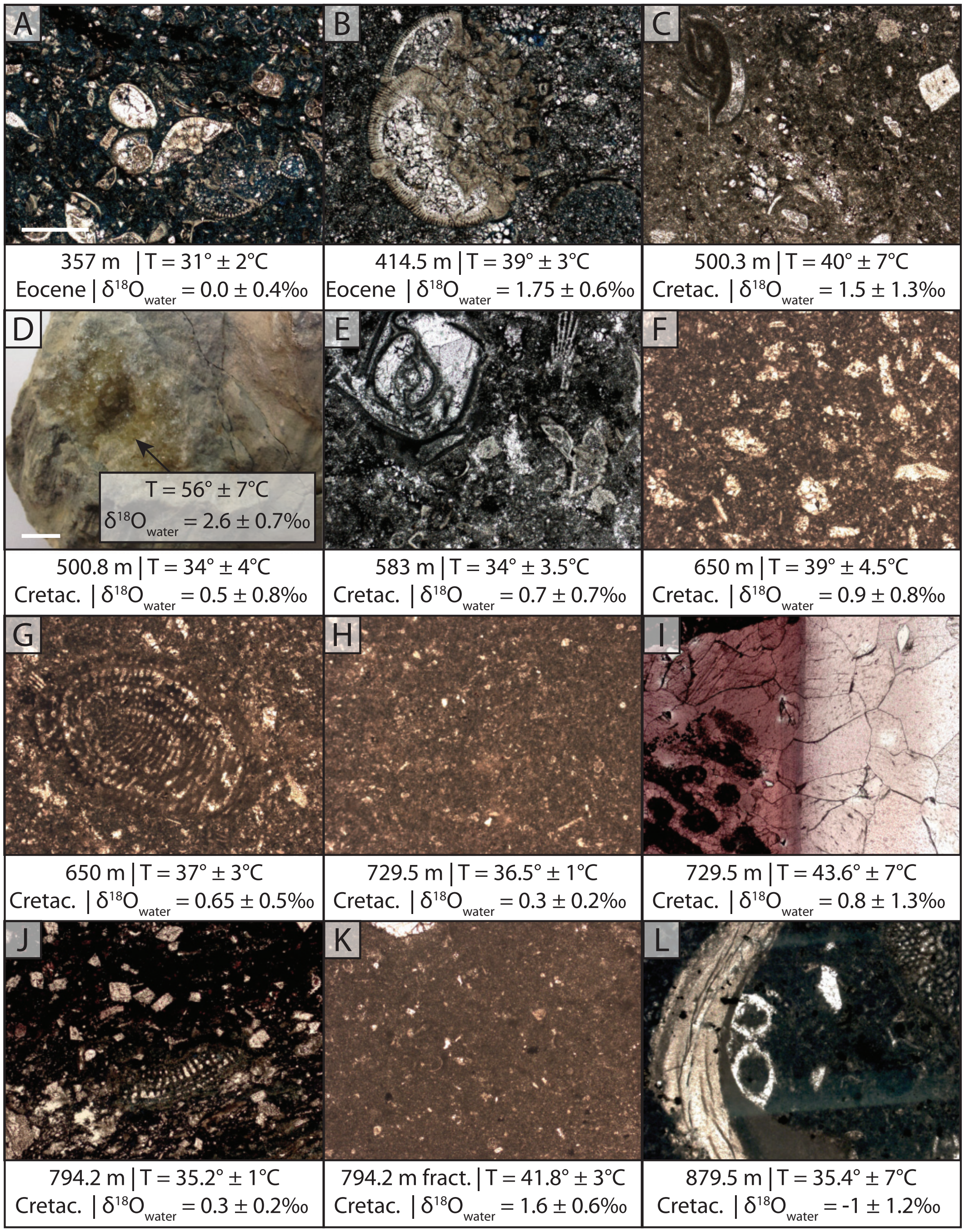

Figure 1.5: Petrographic plate and clumped isotope temperatures for Eocene and Cretaceous aged carbonates. Generally, porosity becomes occluded with depth, the samples with better preserved fossils have lower temperatures. The micro-sampled spar samples are warmer than their surrounding matrix.

Two Jurassic-aged carbonate formations were sampled—the Thuwaiq Mountain and Dhruma formations of the Sahtan Group. The formations are Late Bajocian to Callovian in age. The sample of the Thuwaiq Mountain Formation recovered from 963.2 meters depth is a wackestone with packstone horizons with abundant shell bioclasts in a micrite matrix. Most of the larger shells are completely replaced by calcite spar (HM11) (Fig. 1.7a,b). The sample from the Dhurma Formation recovered from 1038.8 meters depth is a grainstone composed of peloids and the occasional ooid. The porosity is completely occluded with a clear blocky calcite cement (HM12) (Fig. 1.7c).

The Permian-aged Middle and Lower Khuff Formation of the Akhdar Group was also sampled. Four samples from Middle and Lower Khuff recovered from 1114.7, 1198.5, 1264.9 and 1369.7 meters depth are mudstone and lack fossils (HM13, HM14, HM15, HM17) (Fig. 1.7d,e,f,h). HM14, HM15 and HM17 are completely dolomitized. HM17 has high intergranular porosity and HM15 has moderate intergranular porosity as evidenced by the visible blue stained epoxy (Fig. 1.7f,h). Two samples from the Middle and Lower Khuff recovered from 1319.1 and 1420.5 meters depth are grainstone with abundant well-preserved bioclasts cemented with a clear blocky calcite cement (HM16 and HM18) (Fig. 1.7g,i).

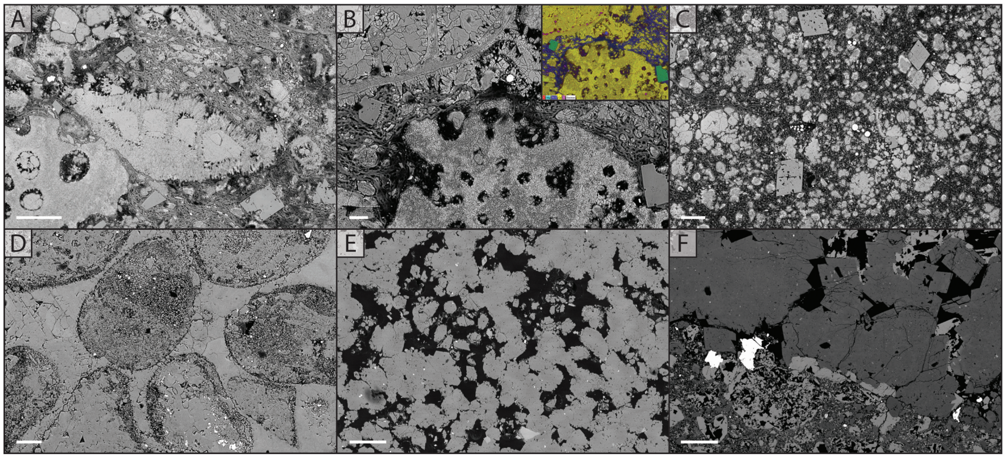

Figure 1.6: SEM images and elemental maps of clumped isotope samples. a. HM1. Scale bar is 100 μm. b. HM1. Scale bar is 20 μm. c. HM4. Scale bar is 40 μm. d. HM12. Scale bar is 40 μm. e. HM15. Scale bar is 40 μm. f. HM20. Scale bar is 200 μm.

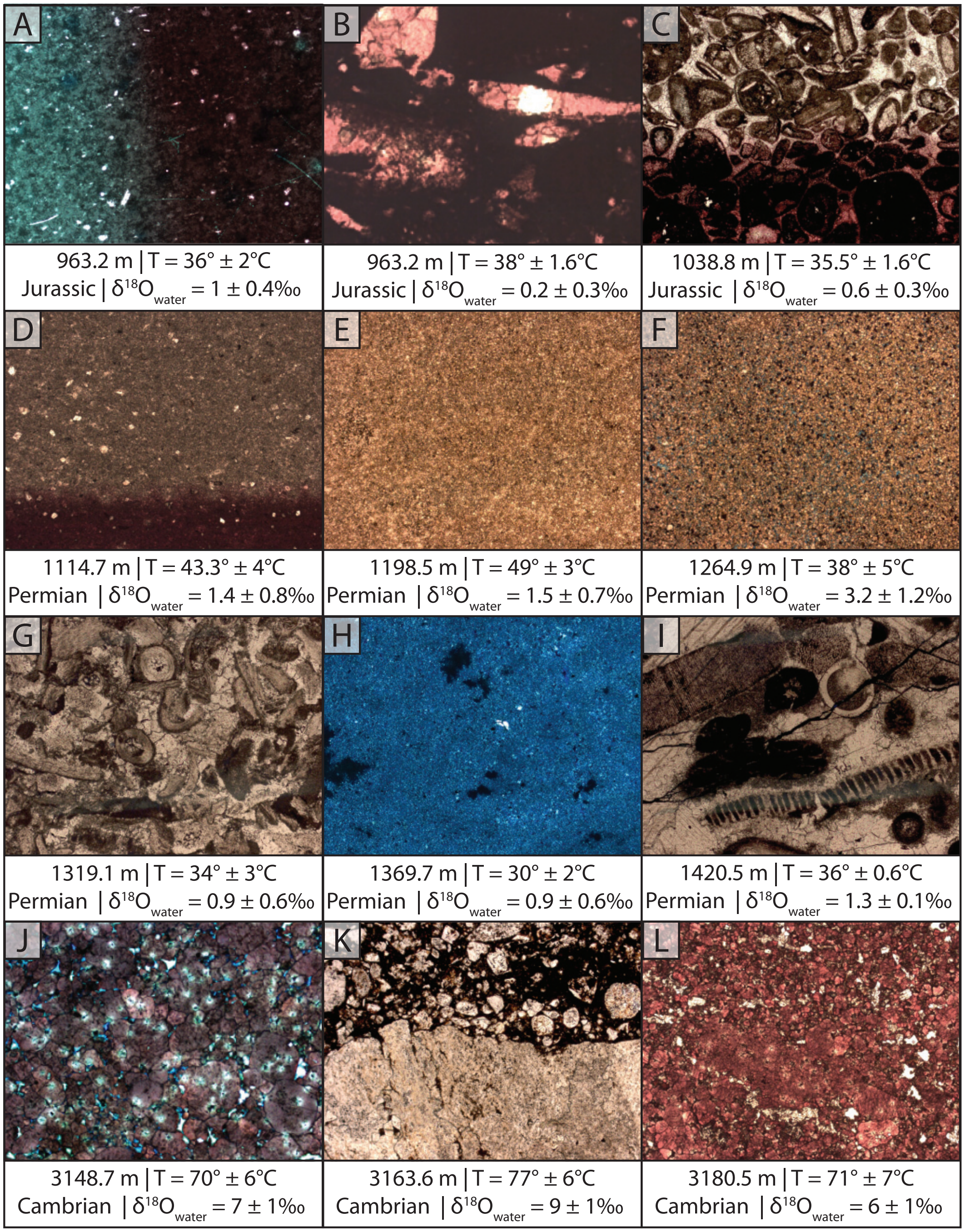

A: 963.2 m | T = 36° ± 2°C
Jurassic | $\delta^{18}O_{water}$ = 1 ± 0.4‰

B: 963.2 m | T = 38° ± 1.6°C
Jurassic | $\delta^{18}O_{water}$ = 0.2 ± 0.3‰

C: 1038.8 m | T = 35.5° ± 1.6°C
Jurassic | $\delta^{18}O_{water}$ = 0.6 ± 0.3‰

D: 1114.7 m | T = 43.3° ± 4°C
Permian | $\delta^{18}O_{water}$ = 1.4 ± 0.8‰

E: 1198.5 m | T = 49° ± 3°C
Permian | $\delta^{18}O_{water}$ = 1.5 ± 0.7‰

F: 1264.9 m | T = 38° ± 5°C
Permian | $\delta^{18}O_{water}$ = 3.2 ± 1.2‰

G: 1319.1 m | T = 34° ± 3°C
Permian | $\delta^{18}O_{water}$ = 0.9 ± 0.6‰

H: 1369.7 m | T = 30° ± 2°C
Permian | $\delta^{18}O_{water}$ = 0.9 ± 0.6‰

I: 1420.5 m | T = 36° ± 0.6°C
Permian | $\delta^{18}O_{water}$ = 1.3 ± 0.1‰

J: 3148.7 m | T = 70° ± 6°C
Cambrian | $\delta^{18}O_{water}$ = 7 ± 1‰

K: 3163.6 m | T = 77° ± 6°C
Cambrian | $\delta^{18}O_{water}$ = 9 ± 1‰

L: 3180.5 m | T = 71° ± 7°C
Cambrian | $\delta^{18}O_{water}$ = 6 ± 1‰

Figure 1.7: Petrographic plate and clumped isotope temperatures for Jurassic- to Cambrian-aged carbonates. The three dolomite samples (e, f and h) have temperature and fluid compositions that vary with the degree of porosity in the sample (highest porosity = lowest temperature).

1.3.2 Latest Precambrian- to Cambrian-aged Ara Group

The Ara Group, within the Huqf Supergroup, spans the Precambrian-Cambrian boundary and is composed of six 3^{rd}-order evaporite-carbonate cycles (A0/A1–A6) [14, 15, 16]. The Ara Group is broken into 5 formations—the Birba Formation (A0–A3 sequences), 'U' Formation (A4 sequence), Athel Formation (A4 sequence), Al Noor Formation (A5 and the evaporite portion of the A6 sequence), and the Dhahaban Formation (the carbonate portion of the A6 sequence) (Fig. 1.3) [17, 15, 16, 13]. Carbonates were deposited on isolated platforms, low-gradient ramps and in more distal environments of the basin during transgressive to highstand conditions while evaporites were deposited during relative lowstand conditions on the platforms and in surrounding basinal environments. The Ara Group is found in the South Oman Salt Basin, the Ghaba Salt Basin and the Fahud Salt Basin. On the eastern margin of the South Oman Salt Basin, on what is termed the Eastern Flank, and towards the Central Oman High in the Northern Carbonate Domain, intra-carbonate evaporites pinch out into a thick sequence of platform carbonates equivalent to the Birba Formation (A0–A3). The carbonate platform of the Eastern Flank is blanketed by a thick evaporite unit thought to be equivalent to the A5/A6 [13]. Subsidence on the Eastern Flank platform must have either been high enough to continue carbonate production through lowstand conditions or low enough that exposure and karst surfaces are equivalent to the evaporite deposits of the South Oman Salt Basin. Additionally, carbonates from a series of Salt Domes sourcing the Ghaba Salt Basin are correlated with the Ara Group [13, 17].

The Ara Group sample suite includes limestone samples from the Dhahaban Formation from the same well the Phanerozoic samples are from (HM19, 20, 21 from 3148.7 meters depth to 3180.5 meters depth) (Fig. 1.7j,k,l). HM19, 20 and 21 are all significantly recrystallized and are mostly calcite with some dolomitization. The samples also have significant amounts of anhydrite. Additional samples are from carbonate 'stringers' encased in salt from the SOSB (A2–A4). Most of these samples are dolomitized but there are a few calcite samples as well. A range of lithofacies was analyzed including crinkly laminite and planar laminite, massive grainstone, and thrombolites. All of the samples, not from cuttings, are crystalline and can reach crystal sizes of 150 μm (Fig. 1.7). Ara Group samples also include Birba Formation samples from the Eastern Flank and Central Oman High (Fig. 1.11) and limestone samples from the Qarn Alam salt dome that sources the Ghaba Salt Basin.

1.3.3 Ediacaran-aged Nafun Group

The Nafun Group, within the Huqf Supergroup, is the oldest carbonate containing unit in Oman and was deposited after the Cryogenian glacial deposits of the Abu Mahara Group. The unit consists of two large-scale siliciclastic-carbonate cycles of the Masirah Bay and Khufai formations and the Shuram and Buah formations. The carbonates are composed of a wide range of lithofacies from mudstone to grainstone in lithofacies associations that generally define a shallowing upwards pattern in the depositional environment of the two carbonate dominated units—the Khufai and Buah formations. There are no good age constraints within the Nafun Group although the basal Hadash carbonate has been correlated with cap carbonates associated with the Marinoan deglaciation ($\sim$ 630 Ma).

The Nafun Group sample suite is from three subsurface wells and the Huqf Outcrop Area (Fig. 1.11). The samples from the subsurface wells are cuttings. The outcrop samples are from a range of lithofacies and depositional environments. The dolomite samples are from the Khufai and Buah Formations while the limestone samples are mostly from the siliciclastic dominated Shuram Formation and the lowermost Khufai Formation. Generally the petrography of the samples from the Huqf Outcrop Area indicates excellent preservation of primary grains and early cementation. The Lower Khufai Formation is the only part of the stratigraphy with evidence for significant recrystallization.

1.4 Methods

1.4.1 Sample collection and preparation

Carbonate samples from the subsurface were collected from cored intervals where possible and from cuttings. Samples from the Qarn Alam Salt Domes were provided by Said Al-Balushi and Monique Mettraux. Samples of the Nafun Group were collected from the Huqf outcrop area in central Oman. Hand samples were cut to expose an unweathered face prior to further analysis. We targeted a range of carbonate facies to improve understanding of preservation biases associated with specific carbonate textures and different primary porosities that lead to varying contributions from secondary cements.

1.4.2 Carbonate clumped isotope thermometry

Samples were analyzed over the period of Jan, 2009-Jan, 2013. Samples were either drilled from a thin-section billet or from a cut slab with a 3 mm rotary drill bit. Rock cuttings were rinsed to remove drilling mud, dried and powdered in a mortar and pestle. 9–12 mg of powder was weighed into silver capsules before being reacted at 90°C in 100% H_3PO_4 in a common acid bath. Evolved CO_2 was purified by multiple cryogenic traps including a Porapak-Q chromatograph held at -20°C before being measured on a ThermoFinnigan MAT 253 IRMS. Methods for the measurement and corrections to analyzed heated gases run during each session following [18, 19]. After corrections based on the heated gas line from a given session and an intercept shift based on the initial calibration experiment, Δ_{47} values were transformed into an absolute reference frame using a secondary transfer function following [20, 21]. The secondary transfer function for each week was calculated using any of the following available data: 25°C and 1000°C CO_2 as well as any of four carbonate standards with known absolute reference frame values (see below). Finally Δ_{47} values for carbonate samples were corrected by $+0.092‰$ for the 90°C acid bath reaction temperature within the absolute reference frame [21].

Values within the absolute reference frame (ARF) for two internal standards used over the course of the analyses, Yale CM (n=35) and TV01 (n=50) were calculated from 7 weeks when 1000°C CO_2 was analyzed daily and 25°C CO_2 gases were analyzed bi-weekly. The calculated values for the two standards in the absolute reference frame are reported with 1 SD for all sessions with heated gases and equilibrated gases: Yale CM (n = 33) Δ_{47}-ARF = 0.404 ± 0.022‰, TV01 (n = 50) Δ_{47}-ARF = 0.730 ± 0.018‰. Absolute reference frame values for two other internal standards run during the analytical period were calculated from weeks where either Yale CM and/or TV01 had been run with them (GC-AZ-01 (n=12) and Carmel Chalk (n=15)). Values are reported with 1 SD for all sessions with heated gases and known standards: 102-GC-AZ01 (n = 12) Δ_{47}-ARF = 0.709 ± 0.023‰, and Carmel Chalk (n=15) Δ_{47}-ARF = 0.678 ± 0.020‰. The values of the Carrara standard and 102-GC-AZ01 in the absolute reference frame are nearly identical to those found at Johns Hopkins (UU Carrara (n = 93) Δ_{47}-ARF = 0.403 ± 0.015‰ and 102-GC-AZ01 (n = 102) Δ_{47}-ARF = 0.710 ± 0.015‰ [21].

The reproducibility of standards for all analytical weeks are reported with 1 SD for all sessions: Yale CM (n = 98) Δ_{47}-ARF = 0.405 ± 0.019‰, 102-GC-AZ01 (n = 23) Δ_{47}-ARF 0.710 ± 0.011‰, TV01 (n = 86) Δ_{47}-ARF 0.730 ± 0.015‰ and Carmel Chalk (n = 17) Δ_{47}-ARF 0.675 ± 0.015‰. For single unknown measurements the uncertainty of the measurement is reported as the standard error of the mean (SEM) of Δ_{47} measurements over 8 acquisitions. For $n \geq 2$, the error is reported as the SEM of Δ_{47} over the number of sample replicates.

Temperatures were calculated in the absolute reference frame as well as the interlab reference frame using the same calibration data from two calibration studies completed at Caltech [22, 1]. To build this calibration equation from low to high temperatures we assume that calcite and dolomite calibrations are equivalent. The two approaches do not yield the exact same temperature on a week to week basis and this is likely due to two factors: 1) conversion of the two calibration studies into the absolute reference frame is imperfect because the samples were analyzed before 25°C CO_2 gases were analyzed regularly and 2) Converting unknown samples into the absolute reference frame using both gases and carbonate standards in the transfer function will correct for standard residuals for a given week.

The mineralogy of each powder analyzed was determined by XRD analysis (see below) to properly calculate the $\delta^{18}O_{min}$ composition using unique 90°C acid digestion fractionation factors for calcite and dolomite [23, 24]. Fluid compositions were calculated using the measured clumped isotope temperatures and separate equilibrium fractionation equations for calcite-water [25] and for dolomite-water [26]. For samples that contained mixtures of calcite and dolomite, the dominant mineralogy was used to calculate $\delta^{18}O_{min}$ and $\delta^{18}O_{water}$. Three different dolomite-water equilibrium fractionation equations were compared [27, 28, 26]. Both [26] and [27] produced $\delta^{18}O_{water}$ results in agreement with co-occurring calcite measurements lending faith in the results. The temperature range of dolomite formation from [26] most closely matched the measured temperature range so it was used to calculate the reported water compositions.

1.4.3 Scanning electron microscopy (SEM)

A ZEISS 1550 VP Field Emission Scanning Electron Microscope (SEM) equipped with an Oxford INCA Energy 300 x-ray Energy Dispersive Spectrometer (EDS) system within the California Institute of Technology Geological and Planetary Sciences Division Analytical Facility was used for high-resolution imaging of each sample. Images were collected at a working distance between 8-9 mm using a Quadrant Back Scattering Detector (QBSD). In addition EDS measurements of individual minerals were made to identify the range of minerals present in a given sample.

1.4.4 Bulk powder x-ray diffraction (XRD)

XRD measurements were made on each powder used for clumped isotope measurements on a PANalytical X'Pert Pro within the Material Science at the California Institute of Technology. Scans were run from 5–70° 2θ with a step size of 0.008 and a scan step time of 10.16 s. A Cu anode was used at 45 kV and 40 mA. A zero-background silicon plate was used for all measurements because of sample size limitations. Mineralogical phases were initially identified using the X'Pert Highscore IDMin function. To determine relative abundances of calcite and dolomite in each sample, the relative peak height intensities of the major calcite and dolomite peaks at 29.5° 2θ and 30.7° 2θ, respectively, were used [29]. Mixtures of known compositions of 100%, 80%, 60%, 40%, 20% and 0% calcite with dolomite were used to create the following relationship of peak height to % dolomite for the PANalytical X'Pert Pro setup at Caltech:

$$PercentDolomite = \frac{\frac{Rel.IntensityofCaMgCO_3}{Rel.IntensityofCaMgCO_3+CaCO_3} - 0.0526}{0.0099} \qquad (1.1)$$

90% of the samples analyzed were pure end-members of either calcite or dolomite. For the 10% of samples that were a mixture of both calcite and dolomite, the acid digestion fractionation for $\delta^{18}O_{min}$ and min-water fractionation factor for all mixtures in the clumped isotope calculations were made assuming 100% composition of the dominant mineralogy. This will introduce a systematic bias for those samples but most are more than 70% one mineralogy. Another approach would be to use the measured CO_2 gas, and use a weighted average to calculate each portion separately. That approach assumes the two phases have the same $\delta^{18}O$ CO_2 gas composition.

1.5 Results

1.5.1 Eocene- to Permian-aged carbonates of Oman

The four samples analyzed from the shallowest burial depth (357 meters) yield a range of temperatures from 30.5° ± 2°C to 38.7° ± 3°C. The lowest temperature sample (HM1) has the highest primary porosity and the smallest amount of secondary calcite spar. The warmest temperature sample (HM2_2) is a diagenetic blocky calcite spar filling the interior of a gastropod shell. The $\delta^{18}O_{min}$ of these four samples is identical at -3.7‰ VPDB while the $\delta^{18}O_{water}$ composition varies from -0.2 ± 0.4‰ VSMOW for the lowest temperature sample to 1.2 ± 0.6‰ VSMOW for the highest temperature spar. Some of these shallow samples have small dolomite rhombs growing within the clay-rich matrix (Fig. 1.6a,b). The Eocene-Paleocene sample from slightly deeper (414.5 meters) yielded a temperature of 38° ± 3°C and a $\delta^{18}O_{water}$ composition of 1.5 ± 0.6‰ VSMOW (Fig. 1.5).

The samples from the Cretaceous and Jurassic demonstrate similar patterns where the three micro-sampled diagenetic cements are the three hottest samples and the only samples > 40°C (40.4° ± 3°C, 42° ± 7°C, 48.6° ± 4°C). In contrast the bulk carbonate drilled from the same samples are between 6-16° cooler (34° ± 1°C, 35° ± 1°C, 32° ± 4°C). Two of the spar samples are approximately 1‰ heavier in $\delta^{18}O_{min}$ composition than the carbonates surrounding them while the other is identical. All three spar samples have enriched $\delta^{18}O_{water}$ composition (1.3 ± 0.6‰, 0.53 ± 1.3‰, 2.4 ± 0.7‰VSMOW). The bulk carbonate drilled from the same samples have $\delta^{18}O_{water}$ compositions near 0‰ (0.05 ± 0.2‰, 0.09 ± 0.2‰, 0.22 ± 0.8‰VSMOW). The sample with visible small dolomite rhombs growing within the sediment is also warmer at 39° ± 7°C with a slightly heavier $\delta^{18}O_{water}$ composition of 1.2 ± 1‰VSMOW. The rest of the samples from the Cretaceous and Jurassic have temperatures that range from 32–37°C and $\delta^{18}O_{water}$ compositions ranging from -1.3–0.7‰VSMOW. While most of the lower temperature samples were wackestone and packstone lithofacies, the one grainstone (HM12) with a significant amount of porosity-occluding clear blocky cement is also in this group (Fig. 1.7c).

The samples from the Permian can be divided into two groups; the dolomitized samples and the calcitic grainstone samples. The three dolomitized samples have very different temperatures (30° ± 2°C, 37° ± 5°C, 48° ± 3°C) that correlate with the porosity of the sample, where the lowest temperature sample has the highest porosity (estimated based on the percentage of blue epoxy showing in thin section). The two calcitic grainstone samples are similar to the younger bulk carbonates (34° ± 1°C, 33° ± 3°C) with $\delta^{18}O_{water}$ compositions of 1 ± 0.2‰and 0.7 ± 0.6‰VSMOW. The $\delta^{18}O_{water}$ compositions of the dolomites (0.9 ± 0.6‰, 3.2 ± 1‰, 1.5 ± 0.7‰VSMOW) are similar to the calcitic samples.

The 3-plot diagrams of temperature, $\delta^{18}O_{min}$, $\delta^{18}O_{water}$ for the Phanerozoic samples can easily distinguish the end-member calcite spar samples and the dolomite samples from the bulk wackestone, packstone and grainstone samples (Fig. 1.8). In general the bulk samples show little modification of their $\delta^{18}O_{water}$ composition as it remains seawater-like in composition.

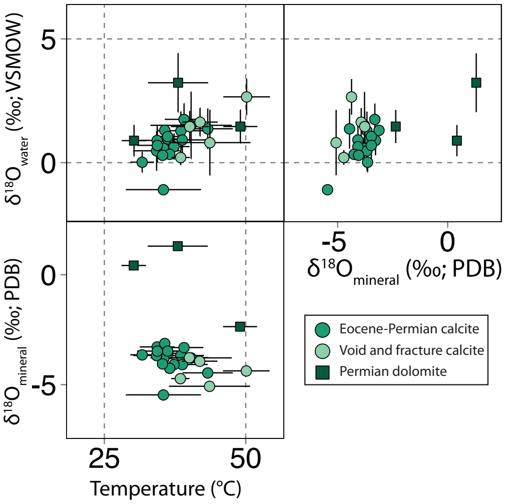

Figure 1.8: 3-plot of clumped isotope temperature, $\delta^{18}O_{min}$, $\delta^{18}O_{water}$ for Eocene- to Permian-aged samples. The samples formed during burial including fracture fills and void filling spar are hotter than the surrounding matrix.

1.5.2 Latest Precambrian- to Cambrian-aged Ara Group

The three samples from the Dhahaban Formation of the Ara Group sampled from the same well that all of the Phanerozoic samples were sampled from (3148.7–3180.5 meters) are markedly different in character. Their temperatures are much higher (67° ± 6°C, 75° ± 5°C, 69° ± 7°C) and their fluid compositions are elevated (7 ± 1‰, 9 ± 0.8‰, 5.5 ± 1‰VSMOW). These temperature and $\delta^{18}O_{water}$ compositions were measured on coarsely recrystallized calcite with evidence for dolomitization that are closely associated with evaporite minerals (Fig. 1.7j,k,l).

Other subsurface samples analyzed from carbonate 'stringers' from various depths in the South Oman Salt Basin yield similarly warm carbonate clumped isotope temperatures. The mean clumped isotope temperature of the Ara Group samples is 81° ± 1.8°C. While the Ara Group samples that are currently 2–4 km depth have temperatures similar to the current measured borehole temperatures there is no statistical difference in the mean clumped isotope temperature of samples buried ~ 2–4 km deep from samples buried 4–6 km deep. The $\delta^{18}O_{water}$ composition of Ara Group samples is highly enriched with a mean of 6.7 ± 0.5‰The bulk samples, whether calcite or dolomite, are highly crystalline and the textures are often interlocking and can be very coarse. There is little difference in the clumped isotope temperatures between calcite and dolomite samples although the calcite samples indicate slightly more enriched $\delta^{18}O_{water}$ compositions of ~ 10‰ (Fig. 1.9).

The Precambrian-Cambrian boundary A4C carbonates are slightly distinct in clumped isotope temperature from the other subsurface Ara Group carbonates. Lithofacies that were analyzed include flat laminite, crinkly laminite, massive fine-grained dolostones and massive coarsely recrystallized dolostones. The mean clumped isotope temperature is slightly lower (69° ± 2.3°C) and the $\delta^{18}O_{water}$ composition is less enriched (2.6 ± 0.4‰ VSMOW).

Samples from the Birba Formation on the Eastern Flank or Central Oman High, that are not floating within salt, are in general slightly cooler than the SOSB Ara Group samples (Fig. 1.9). However, they are warmer in apparent clumped isotope temperature than the underlying Nafun Group carbonates from the same well (Fig. 1.11).

Exhumed Ara Group carbonates from the Qarn Alam Salt Dome that source the Ghaba Salt Basin are similar to the subsurface Ara Group samples from the SOSB but have slightly elevated maximum temperatures (Fig. 1.9). The temperatures range from 67° ± 4°C to 131° ± 31°C. The $\delta^{18}O_{water}$ compositions are enriched and range from 2.8 ± 1‰ to 15 ± 4‰ VSMOW. XRD analyses of the Qarn Alam samples indicate they are predominantly calcite with minor dolomite.

The relationship between temperature, $\delta^{18}O_{min}$ and $\delta^{18}O_{fluid}$ of the Ara Group carbonates indicates these rocks have undergone recrystallization in a low-water/rock environment (Fig. 1.9). At progressively high temperatures, the $\delta^{18}O_{fluid}$ becomes increasingly enriched as the small pore volumes of fluid exchange oxygen with the surrounding carbonates. The diagenetic trajectory indicated by the Ara Group dataset displays a slight curvature, indicating the $\delta^{18}O_{min}$ is largely invariant because the relationship between temperature-water-mineral composition is non-linear (Fig. 1.9).

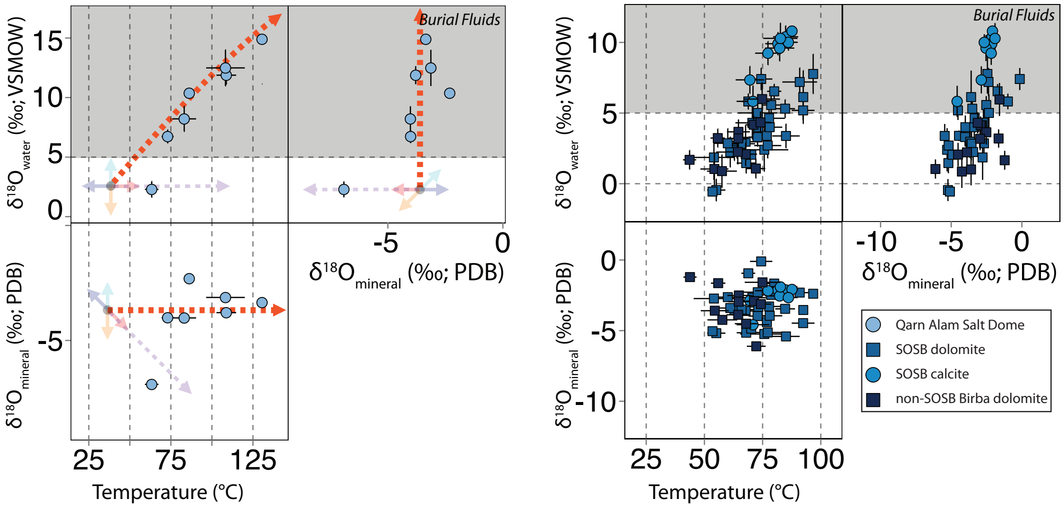

Figure 1.9: 3-plot of clumped isotope temperature, $\delta^{18}O_{min}$, $\delta^{18}O_{water}$ for Ediacaran-Cambrian aged samples from the Ara Group. The Qarn Alam Salt Dome samples sourcing the Ghaba Salt Basin generally show higher temperatures than the SOSB samples. The orange arrow denotes low water/rock ratio diagenesis. The grey shading indicates enriched burial fluids. The Birba carbonates from the Eastern Flank and Central Oman show the lowest temperatures of the Ara Group.

1.5.3 Ediacaran-aged Nafun Group

The samples from the subsurface Nafun Group span a lower range in temperatures than the Ara Group carbonates (43° ± 0.7°C–78° ± 11°C). Exhumed Nafun Group carbonates from the Central Oman High span similar range in temperatures (37° ± 6°C–78° ± 8°C) with most of the population sitting at the lower end of the temperature range. There is a clear difference between calcite and dolomite samples from the Nafun Group carbonates. The calcite samples show a similar trend on a 3-plot diagram to the Ara Group carbonates and we suggest they are more are strongly controlled by low water-rock ratio diagenesis (Fig. 1.10). This is likely because almost all of the calcites were sampled from the siliciclastic dominated Shuram Formation. The burial environment of a fine-grained siltstone is very similar to a salt. The carbonate will have minimal pore fluids surrounding it and water-rock interactions will end up rock buffered (Fig. 1.10). The dolomite samples display a very different pattern in the 3-plot diagram. Most of the data occupies a narrow range in temperature but span a wide range of fluid compositions. This range in fluid compositions is likely a reflection of the wide range of depositional environments these carbonates were deposited in—from shallow subtidal through peritidal into restricted lagoonal and supratidal environments.

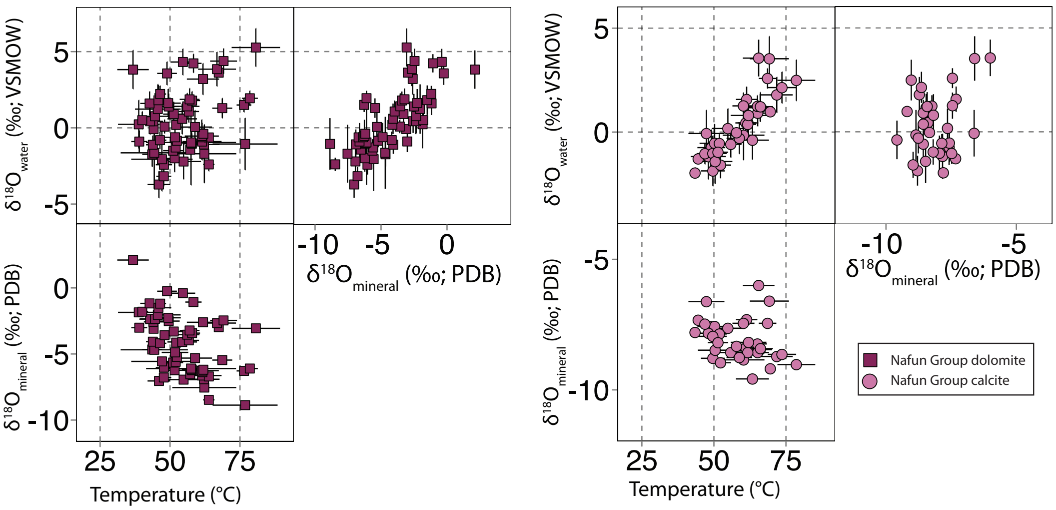

Figure 1.10: 3-plot of clumped isotope temperature, $\delta^{18}O_{min}$, $\delta^{18}O_{water}$ for Ediacaran-aged samples from the Nafun Group. The dolomite samples from the Nafun Group generally have a small range in temperature (40–60°C) but show a large range in fluid compositions. The calcite samples from the Nafun Group (almost all are from within the Shuram Formation) demonstrate low-water rock ratio diagenesis.

1.6 Discussion

These results indicate two important modes of diagenesis in marine burial environments. Low water-rock ratio regimes dominate in burial environments with limited fluid flow. A good example of this type is seen in the carbonates hosted in Salt Basin evaporites. Another example is the calcite samples from the Nafun Group which are predominantly thin carbonates within thick siltstone, a burial environment not unlike the carbonate-salt environment in many ways. This diagenetic regime is contrasted with the high water/rock regime. This style of diagenesis appears to occlude porosity very early because the fluid compositions remain buffered near seawater values (Fig. 1.11). Samples that depart from this trend in the Phanerozoic are micro-sampled calcite spar from veins and cavities.

Given the tectonic setting and location of the subsurface samples either on the Central Oman High or in the South Oman Salt Basin, we assume the current burial depth is likely the maximum burial depth for most samples. The Phanerozoic samples analyzed demonstrate that diagenetic end-member components including calcite spar have higher temperatures than the bulk carbonates surrounding them (Fig. 1.8). They also indicate that over a depth range of 357–1420 meters the carbonate clumped isotope temperatures of Eocene- to Permian-aged bulk carbonates are very similar with a mean of 35° ± 2.6°C (1 SD). The $\delta^{18}O_{water}$ compositions show very little deviation with a mean of 0.5 ± 0.6‰ VSMOW (1 SD). Importantly, carbonates that are buried $\sim$ 1.5 km at geothermal temperatures of $\sim$ 70°C (present day) for hundreds of millions of years have similar temperature and fluid compositions as Eocene-aged carbonates buried 450 meters. These bulk carbonates show very little diagenetic spread on a 3-plot diagram. Co-occurring calcite spar sampled from specific depths (357.1, 500.8, 729.5, 794.2) sit much closer to the borehole temperature from the bulk carbonate samples from those respective depths.

The Ara Group carbonates have recrystallized at much higher temperatures that approach the current borehole temperatures in the subsurface samples buried

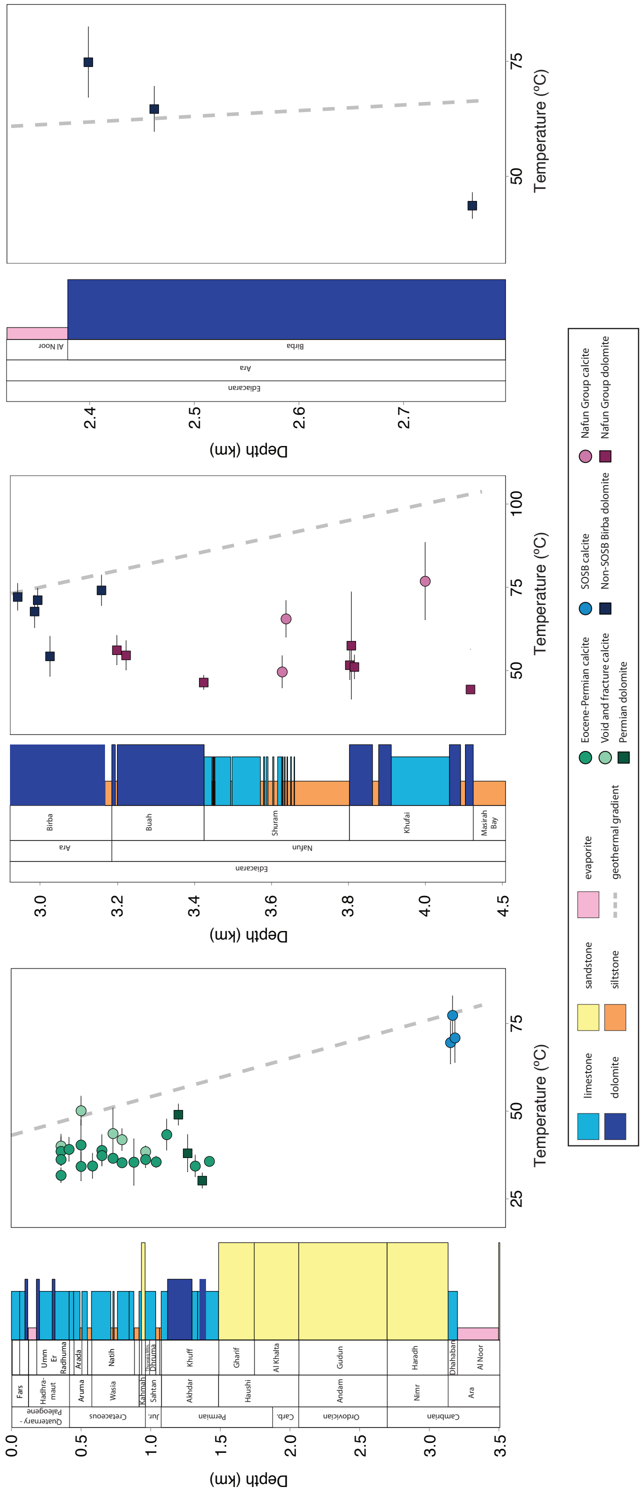

Figure 1.11: Clumped isotope temperatures versus depth with the measured borehole geothermal gradient for three subsurface wells. Only the Ara Group carbonates (both calcite and dolomite) sit on the current geotherm.

2-4 km deep. The samples indicate significant low water/rock recrystallization has occurred which is supported by the fine to coarsely crystalline nature of most samples. More sections of the A4C carbonate need to be analyzed to determine if the cooler temperatures and less enriched fluid compositions is a basin-wide pattern (Fig. 1.9). The diagenetic character of the Ara Group is likely strongly controlled by the depositional environment of a mixed carbonate-evaporite setting. The carbonate ’stringers’ as they are termed now float within the salt. The pore fluids associated with these carbonates are highly evolved and support long-term isolation. The Birba Formation carbonates from the Eastern Flank and Central Oman High also sit on the present day geothermal gradient in their given well unlike the underlying Nafun Group.

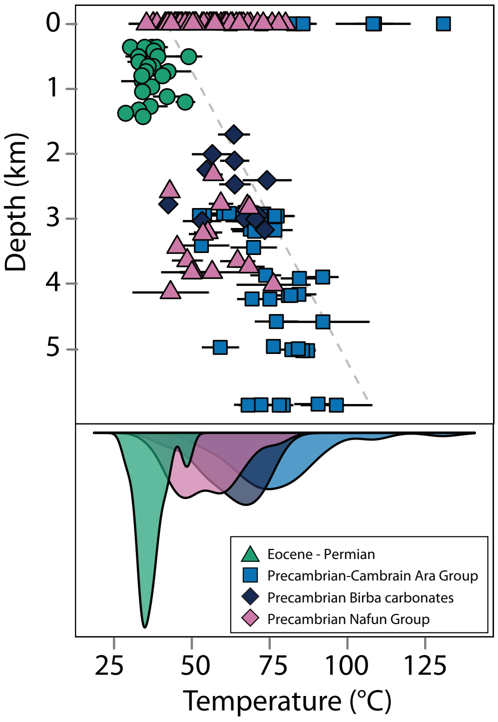

Figure 1.12: Clumped isotope temperatures versus depth with a generalized geothermal gradient for Central and Southern Oman. Only the Ara Group carbonates (both calcite and dolomite) sit on the current geotherm.

The Nafun Group carbonates resemble the Phanerozoic carbonates in many ways. The petrographic fabrics are similar and the $\delta^{18}O_{water}$ composition is overlapping (Fig. 1.13). Yet the temperatures that yield $\delta^{18}O_{water}$ compositions of $\sim$ 0‰ are generally 5–10°C warmer (Fig. 1.10). The samples from the carbonate dominated Khufai and Buah formations likely underwent similar processes of porosity occlusion and cementation early in their history like the Phanerozoic samples because the $\delta^{18}O_{w}ater$ composition is so similar to seawater. This likely due to similar carbonate-dominated burial environments that are fluid rich during burial.

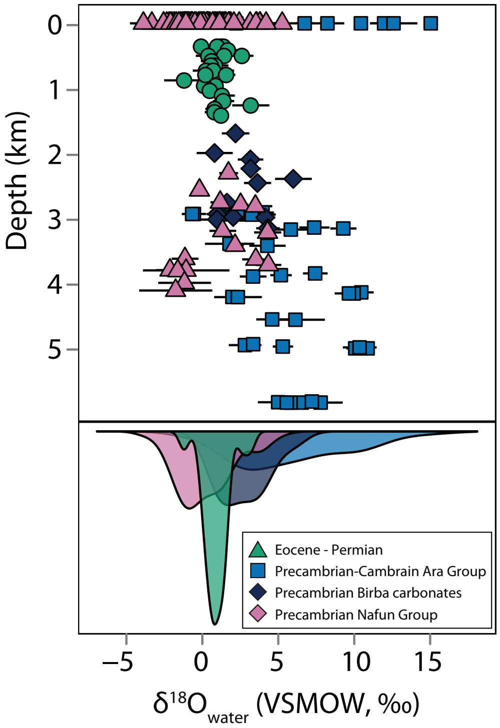

Figure 1.13: $\delta^{18}O_{water}$ versus depth for Central and Southern Oman. Both the Eocene- to Permian-aged carbonates and the Nafun Group carbonates yield $\delta^{18}O_{water}$ compositions of $\sim$ 0‰. The Ara Group carbonates yield strongly enriched fluid compositions.

These results suggest that in shallow burial environments (0–$\sim$ 5 km) there is a population that has undergone early burial diagenesis controlled by marine pore waters and a population that has undergone later burial diagenesis with evolved formation waters (Fig. 1.12). There is likely some increase in the measured clumped isotope temperature in the early burial diagenesis population from mixing in secondary calcite cements however there appear to be clear differences between

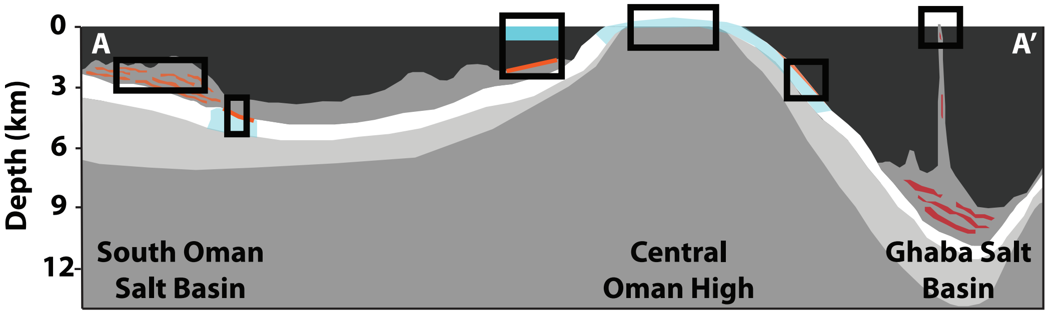

Figure 1.14: Schematic model of clumped isotope thermometry behavior in South and Central Oman. The Ara Group carbonates whether in the SOSB, Central Oman (orange) or Ghaba Salt Basin (red) have temperatures similar to the current geothermal gradient temperatures and enriched fluid compositions. Most other bulk carbonates yield $\delta^{18}O_{water}$ compositions suggesting they cemented within the shallow subsurface and have not been strongly altered since (light blue).

bulk carbonates (i.e., grainstone) that are composed of up to 30% clear blocky cements and calcite cements that fill cavities and veins. This suggests much of the blocky calcite found in carbonate grainstone facies is a very early phase. The bulk carbonates that yield clumped isotope temperatures approaching the current geothermal gradient tend to be in environments with low water/rock ratios. While more studies of this kind should be done on natural samples from a range of borehole depths, these data do not support significant 'solid state reordering' in the shallow burial environment. Instead, the results can be explained based on recrystallization history and petrographic differences as well as burial environment.

1.7 Conclusion

Clumped isotope analyses of carbonates from the subsurface spanning a wide range of depths (450 meters–∼ 6 km), indicate that only a few carbonate have temperatures that reflect the geothermal gradient. These carbonates tend to either be later diagenetic cements and veins or are found in environments that have very low surrounding porosities (i.e., the Ara Group). In contrast, the Phanerozoic and Nafun Group samples from a carbonate dominated system yield clumped isotope temperatures that likely reflect near-surface temperatures where the various components of these rocks precipitated in equilibrium with seawater. These results suggest solid state diffusion is not a dominant process in shallow burial environments on geologic timescales [5]. The study can be more broadly applied to suggest many bulk carbonates reflect near primary conditions and are stabilized early in their history. Late burial diagenetic processes can be easily distinguished from this early stabilization.

1.8 Acknowledgements

We would like to thank Petroleum Development Oman for providing samples and subsurface borehole temperature data. Specifically Gideon Lopes Cardozo, Zuwena Al Rawahi and Joachim Amthor supported multiple aspects of this project through its conception and implementation. Petroleum Development Oman, the Agouron Institute and NASA Astrobiology Institute contributed to analytical costs. We would like to thank Maggie Osburn for fieldwork assistance related to sampling the Nafun Group in the Huqf Outcrop Area. We would also like to thank Nami Kitchen and Chi Ma for analytical assistance. A National Science Foundation Graduate Research Fellowship was provided to K. Bergmann.

References

[1] P. Ghosh, J. Adkins, H. Affek, B. Balta, W.F. Guo, E.A. Schauble, D. Schrag, and J.M. Eller. C-13-O-18 bonds in carbonate minerals: A new kind of paleothermometer. *Geochimica Et Cosmochimica Acta*, 70(6):1439–1456, 2006.

[2] E.A. Schauble, P. Ghosh, and J.M. Eiler. Preferential formation of C-13-O-18 bonds in carbonate minerals, estimated using first-principles lattice dynamics. *Geochimica Et Cosmochimica Acta*, 70(10):2510–2529, 2006.

[3] R.E. Came, J.M. Eiler, J. Veizer, K. Azmy, U. Brand, and C.R. Weidman. Coupling of surface temperatures and atmospheric CO2 concentrations during the Palaeozoic era. *Nature*, 449(7159):198–U193, 2007.

[4] J.M. Eiler. "clumped-isotope" geochemistry - the study of naturally-occurring, multiply-substituted isotopologues. *Earth and Planetary Science Letters*, 262(3-4):309–327, 2007.

[5] B.H. Passey and G.A. Henkes. Carbonate clumped isotope bond reordering and geospeedometry. *Earth and Planetary Science Letters*, 351:223–236, 2012.

[6] J.M. Ferry, B.H. Passey, C. Vasconcelos, and J.M. Eiler. Formation of dolomite at 40-80 degrees c in the Latemar carbonate buildup, dolomites, Italy, from clumped isotope thermometry. *Geology*, 39(6):571–574, 2011.

[7] S. Finnegan, K. Bergmann, J.M. Eiler, D.S. Jones, D.A. Fike, I. Eisenman, N.C. Hughes, A.K. Tripati, and W.W. Fischer. The magnitude and duration of Late Ordovician-Early Silurian glaciation. *Science*, 331(6019):903–906, 2011.

[8] K.E. Snell, J.M. Eiler, D. Dettman, and P.L. Koch. Continental temperatures from the Paleocene-Eocene boundary in the Big Horn Basin, WY from carbonate clumped isotope thermometry. *Geochimica Et Cosmochimica Acta*, 71(15):A950–A950, 2007.

[9] K.W. Huntington, B.P. Wernicke, J.M. Eiler, and R.M. Flowers. Temperature and timing of diagenesis from carbonate clumped isotope thermometry and thermochronology. *Geochimica Et Cosmochimica Acta*, 72(12):A403–A403, 2008.

[10] J.M. Eiler, M. Bonifacie, and M. Daeron. 'clumped isotope' thermometry for high-temperature problems. *Geochimica Et Cosmochimica Acta*, 73(13):A322–A322, 2009.

[11] K.W. Huntington, D.A. Budd, B.P. Wernicke, and J.M. Eiler. Use of clumped-isotope thermometry to constrain the crystallization temperature of diagenetic calcite. *Journal of Sedimentary Research*, 81(9):656–669, 2011.

[12] E.M. Swanson, B.P. Wernicke, J.M. Eiler, and S. Losh. Temperatures and fluids on faults based on carbonate clumped-isotope thermometry. *American Journal of Science*, 312(1):1–21, 2012.

[13] G.A. Forbes, H.S.M. Jansen, and J. Schreurs. Lexicon of Oman: Subsurface stratigraphy. *Reference Guide to the Stratigraphy of Oman's Hydrocarbon Basins*, pages 1–373, 2010.

[14] B.W. Mattes and S.C. Morris. Carbonate evaporite deposition in the Late Precambrian - Early Cambrian Ara Formation of Southern Oman. *Geology and Tectonics of the Oman Region*, 49:617–636 845, 1990.

[15] S. Schroder, B.C. Schreiber, J.E. Amthor, and A. Matter. A depositional model for the terminal Neoproterozoic Early Cambrian Ara Group evaporites in south Oman. *Sedimentology*, 50(5):879–898, 2003.

[16] S. Schroder, J.P. Grotzinger, J.E. Amthor, and A. Matter. Carbonate deposition and hydrocarbon reservoir development at the Precambrian-Cambrian boundary: The Ara Group in South Oman. *Sedimentary Geology*, 180(1-2):1–28, 2005.

[17] H.A. Al-Siyabi. Exploration history of the Ara intrasalt carbonate stringers in the South Oman Salt Basin. *Geoarabia*, 10(4):39–72, 2005.

[18] K.W. Huntington, J.M. Eiler, H.P. Affek, W. Guo, M. Bonifacie, L.Y. Yeung, N. Thiagarajan, B. Passey, A. Tripati, M. Daeron, and R. Came. Methods and limitations of 'clumped' CO2 isotope (Delta(47)) analysis by gas-source isotope ratio mass spectrometry. *Journal of Mass Spectrometry*, 44(9):1318–1329, 2009.

[19] B.H. Passey, N.E. Levin, T.E. Cerling, F.H. Brown, and J.M. Eiler. High-temperature environments of human evolution in East Africa based on bond ordering in paleosol carbonates. *Proceedings of the National Academy of Sciences of the United States of America*, 107(25):11245–11249, 2010.

[20] K.J. Dennis, H.P. Affek, B.H. Passey, D.P. Schrag, and J.M. Eiler. Defining an absolute reference frame for 'clumped' isotope studies of CO2. *Geochimica Et Cosmochimica Acta*, 75(22):7117–7131, 2011.

[21] G.A. Henkes, B. Passey, A.D. WaNamaker, E.L. Grossman, W.G. Ambrose, and M.L. Carroll. Carbonate clumped isotope compositions of modern marine mollusk and brachiopod shells. *Geochimica Et Cosmochimica Acta*, 106(1):307–325, 2013.

[22] M. Bonifaci and J. Eiler. High temperature dolomite calibration. inpress.

[23] J. Rosenbaum and S.M.F. Sheppard. An isotopic study of siderites, dolomites and ankerites at high-temperatures. *Geochimica Et Cosmochimica Acta*, 50(6):1147–1150, 1986.

[24] P.K. Swart, S.J. Burns, and J.J. Leder. Fractionation of the stable isotopes of oxygen and carbon in carbon-dioxide during the reaction of calcite with phosphoric-acid as a function of temperature and technique. *Chemical Geology*, 86(2):89–96, 1991.

[25] S.T. Kim and J.R. Oneil. Equilibrium and nonequilibrium oxygen isotope effects in synthetic carbonates. *Geochimica Et Cosmochimica Acta*, 61(16):3461–3475, 1997.

[26] C. Vasconcelos, J.A. McKenzie, R. Warthmann, and S.M. Bernasconi. Calibration of the delta O-18 paleothermometer for dolomite precipitated in microbial cultures and natural environments. *Geology*, 33(4):317–320, 2005.

[27] A. Matthews and A. Katz. Oxygen isotope fractionation during dolomitization of calcium-carbonate. *Geochimica Et Cosmochimica Acta*, 41(10):1431–1438, 1977.

[28] M. Schmidt, S. Xeflide, R. Botz, and S. Mann. Oxygen isotope fractionation during synthesis of CaMg-carbonate and implications for sedimentary dolomite formation. *Geochimica Et Cosmochimica Acta*, 69(19):4665–4674, 2005.

[29] C.B. Tennant and R.W. Berger. X-ray determination of dolomite-calcite ratio of a carbonate rock. *American Mineralogist*, 42(1-2):23–29, 1957.